



## Isotopic dependence of the pygmy dipole resonance

N. Paar<sup>a</sup>, T. Nikšić<sup>b,c</sup>, D. Vretenar<sup>b,c</sup>, P. Ring<sup>c</sup>

<sup>a</sup> *Institut für Kernphysik, Technische Universität Darmstadt, Schlossgartenstr. 9, D-64289 Darmstadt, Germany*

<sup>b</sup> *Physics Department, Faculty of Science, University of Zagreb, Croatia*

<sup>c</sup> *Physik-Department der Technischen Universität München, D-85748 Garching, Germany*

Received 8 August 2004; received in revised form 2 December 2004; accepted 4 December 2004

Available online 10 December 2004

Editor: J.-P. Blaizot

### Abstract

The isotopic dependence of the excitation energies of the pygmy dipole resonance (PDR) is analyzed in the framework of the self-consistent relativistic Hartree–Bogoliubov (RHB) model and the relativistic quasiparticle random-phase approximation (RQRPA). The DD-ME1 density-dependent meson-exchange interaction is used in the effective mean-field Lagrangian, and pairing correlations are described by the pairing part of the finite-range Gogny interaction D1S. Model calculations reproduce available experimental data on charge radii, the neutron skin, neutron separation energies, and excitation energies of isovector giant dipole resonances in Ni, Sn and Pb nuclei. In all three isotopic chains the one-neutron separation energies decrease with mass number much faster than the excitation energies of the PDR. As a result, already at moderate proton–neutron asymmetry the PDR peak energy is calculated above the neutron emission threshold. This result has important implications for the observation of the PDR in ( $\gamma$ ,  $\gamma'$ ) experiments.

© 2004 Elsevier B.V. All rights reserved.

PACS: 21.10.Gv; 21.30.Fe; 21.60.Jz; 24.30.Cz

Studies of the structure and stability of nuclei with extreme isospin values provide new insights into every aspect of the nuclear many-body problem. In neutron-rich nuclei far from the valley of  $\beta$ -stability, in particular, new shell structures occur as a result of the modification of the effective nuclear potential. Neutron density distributions become very diffuse and the phenomenon of the evolution of the neutron skin and,

in some cases, the neutron halo have been observed. The weak binding of outermost neutrons gives rise to soft excitation modes. In particular, the pygmy dipole resonance (PDR), i.e., the resonant oscillation of the weakly-bound neutron mantle against the isospin saturated proton–neutron core, has recently been the subject of a number of theoretical and experimental studies. Its structure, however, remains very much under discussion. Properties of the PDR in neutron-rich nuclei have important implications on theoretical pre-

*E-mail address:* [nils.paar@physik.tu-darmstadt.de](mailto:nils.paar@physik.tu-darmstadt.de) (N. Paar).

dictions of the radiative neutron capture rates in the r-process nucleosynthesis, and consequently to the calculated elemental abundance distribution [1–3]. Furthermore, the detailed knowledge of the structure of low-energy modes of excitation would also place stringent constraints on the isovector channel of effective nuclear interactions. An interesting problem is the isotopic dependence of the PDR, and especially the behavior of the PDR in the vicinity of major spherical shell gaps. Already in a recent study of low-lying  $2^+$  excitations in the region of the  $N = 82$  magic neutron number [4], it has been observed that the lowering of the first excited  $2^+$  state in neutron-rich Te isotopes is accompanied by a reduction of the corresponding E2 strength, in contradiction with systematics and general expectations about quadrupole collectivity. The anomalous behavior of the Te isotopes has been explained by the weakening of neutron pairing above the  $N = 82$  spherical gap [5].

A systematic analysis of the dipole response of light exotic nuclei has been recently reported in the experimental study of electromagnetic excitations of oxygen isotopes in heavy-ion collisions [6]. For neutron-rich oxygen isotopes the resulting photo-neutron cross sections are characterized by a pronounced concentration of low-lying E1 strength. The onset of low-lying E1 strength has been observed not only in exotic nuclei with a large neutron excess, but also in stable nuclei with moderate proton–neutron asymmetry. High resolution photon scattering has been employed to measure low-lying dipole strength distributions in Ca [7], Sn [8] and Pb [9,10] isotopes, and in the  $N = 82$  [11] isotone chain.

A number of theoretical approaches have been employed in the investigation of the nature of the low-lying dipole strength: the Steinwedel–Jensen hydrodynamical model [12], density functional theory [13], large-scale shell-model calculations [14], the self-consistent Skyrme Hartree–Fock + RPA model [15], Skyrme Hartree–Fock + QRPA with phonon coupling [16], time-dependent density-matrix theory [17], continuum linear response in the coordinate-space Hartree–Fock–Bogoliubov formalism [18], the quasiparticle phonon model [9,10,19,20], the relativistic RPA [21], and the relativistic QRPA in the canonical basis of the relativistic Hartree–Bogoliubov model [22]. In general, the dipole response of very neutron-rich isotopes is characterized by the fragmentation of

the strength distribution and its spreading into the low-energy region, and by the mixing of isoscalar and isovector modes. In relatively light nuclei the onset of dipole strength in the low-energy region is due to nonresonant independent single particle excitations of the loosely bound neutrons. However, the structure of the low-lying dipole strength changes with mass. As we have shown in the RPA analysis of Ref. [21], in heavier nuclei low-lying dipole states appear that are characterized by a more distributed structure of the RPA amplitude. Among several peaks characterized by single particle transitions, a single collective dipole state is identified below 10 MeV, and its amplitude represents a coherent superposition of many neutron particle–hole configurations.

In this work we use the relativistic quasiparticle random phase approximation (RQRPA) based on the canonical single-nucleon basis of the relativistic Hartree–Bogoliubov (RHB) model, to analyze the isotopic dependence of dipole pygmy resonances in medium-heavy and heavy nuclei. The RHB model provides a unified description of particle–hole ( $ph$ ) and particle–particle ( $pp$ ) correlations. In the canonical basis, in particular, the ground state of a nucleus takes the form of a highly correlated BCS-state. By definition, the canonical basis diagonalizes the density matrix and is always localized. It describes both the bound states and the positive-energy single-particle continuum. The formulation of the RQRPA in the canonical basis is particularly convenient because, in order to describe transitions to low-lying excited states in weakly bound nuclei, the two-quasiparticle configuration space must include states with both nucleons in the discrete bound levels, states with one nucleon in a bound level and one nucleon in the continuum, and also states with both nucleons in the continuum.

The relativistic QRPA of Ref. [22] is fully self-consistent. For the interaction in the particle–hole channel effective Lagrangians with nonlinear meson self-interactions or density-dependent meson–nucleon couplings are used, and pairing correlations are described by the pairing part of the finite-range Gogny interaction. Both in the  $ph$  and  $pp$  channels, the same interactions are used in the RHB equations that determine the canonical quasiparticle basis, and in the matrix equations of the RQRPA. This feature is essential for the decoupling of the zero-energy mode which corresponds to the spurious

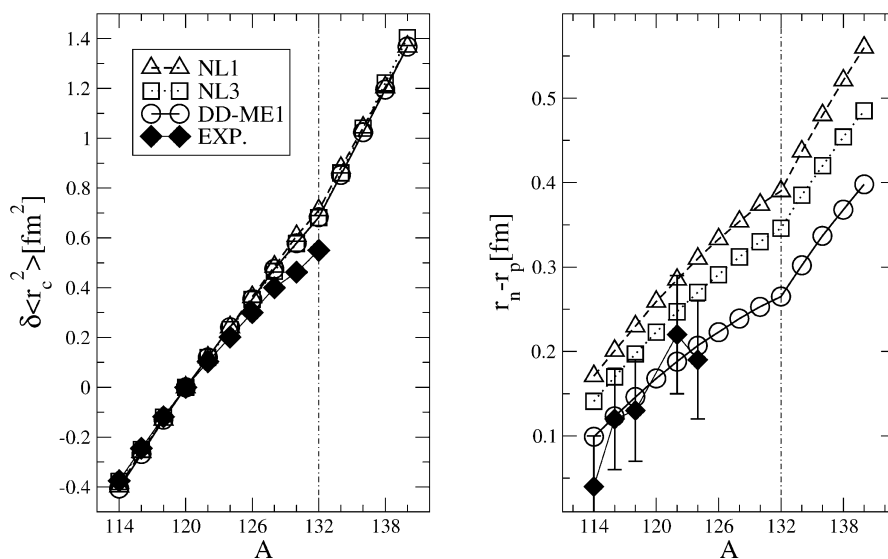


Fig. 1. Charge isotope shifts (left panel), and the differences between the radii of neutron and proton density distributions (right panel) for the Sn isotopes, as functions of the mass number. The values calculated in the RHB model with the NL1, NL3 and DD-ME1 effective interactions, are shown in comparison with empirical data [31–33].

center-of-mass motion. In addition to configurations built from two-quasiparticle states of positive energy, the RQRPA configuration space contains quasiparticle excitations formed from the ground-state configurations of fully or partially occupied states of positive energy and the empty negative-energy states from the Dirac sea.

The R(Q)RPA model has been successfully employed in analyses of low-lying quadrupole and dipole states [21,22], multipole giant resonances [23], toroidal dipole resonances [24], isobaric analog and Gamow–Teller resonances [25]. In Ref. [26] we have extended the RRPA framework to include relativistic effective mean-field interactions with density-dependent meson–nucleon couplings. In a number of recent studies it has been shown that, in comparison with standard RMF effective interactions with nonlinear meson-exchange terms, density-dependent meson–nucleon interactions significantly improve the description of asymmetric nuclear matter and isovector ground-state properties of finite nuclei. This is, of course, very important for the extension of RMF-based models to exotic nuclei far from  $\beta$ -stability. In particular, one expects that the properties of pygmy modes will be closely related to the size of the neutron skin [19] and, therefore, in a quantitative analysis it is

important to use effective interactions that reproduce available data on the neutron skin.

In the present study the density-dependent effective interaction DD-ME1 [27] is employed in the RQRPA calculation of the dipole response in the Sn, Ni and Pb isotopic chains. In Fig. 1 we display the self-consistent RHB model results for the charge isotope shifts and the differences between the radii of the neutron and proton density distributions of Sn isotopes. The Gogny interaction D1S [28] is used in the pairing channel, and the radii calculated with the DD-ME1 interaction, and with two standard nonlinear effective interactions NL1 [29] and NL3 [30], are shown in comparison with available empirical data [31–33]. Although the charge radii calculated with all three effective interactions are in very good agreement with experimental data, only DD-ME1 quantitatively reproduces the evolution of the neutron skin. Because of their high asymmetry energy at saturation density, NL1 and NL3 predict much larger neutron radii. A high value of the asymmetry energy characterizes all the standard RMF forces with nonlinear meson-exchange terms and, therefore, large neutron radii are obtained with any of these interactions. In the following analysis we employ the RHB + RQRPA model with the density-dependent interaction DD-ME1 in the  $ph$ -channel,

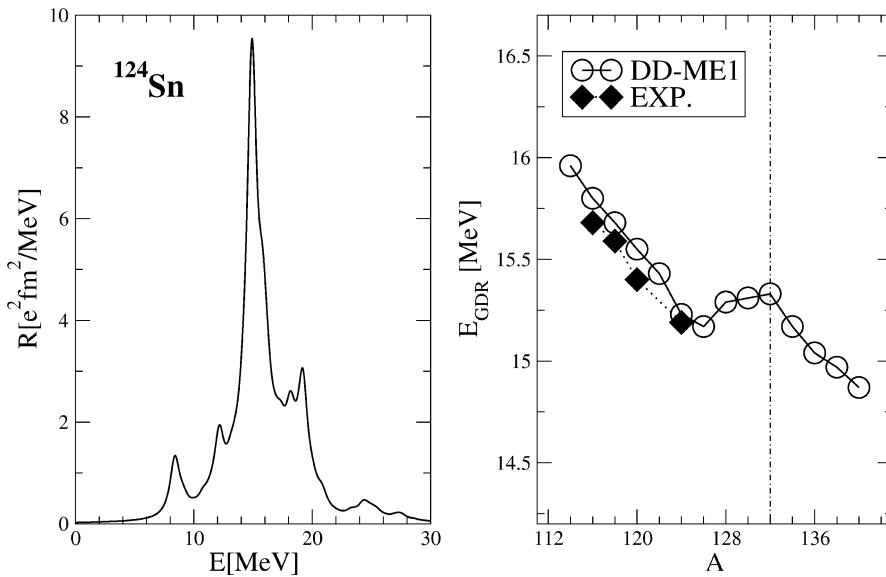


Fig. 2. The RHB + RQRPA isovector dipole strength distribution in  $^{124}\text{Sn}$  (left panel). The experimental IV GDR excitation energies for the Sn isotopes are compared with the RHB + RQRPA results calculated with the DD-ME1 effective interaction (right panel).

and with the finite range Gogny interaction DIS in the  $pp$ -channel.

In Fig. 2 we display the isovector dipole strength distribution in  $^{124}\text{Sn}$ . The calculation is fully self-consistent, with the Gogny finite-range pairing included both in the RHB ground state, and in the RQRPA residual interaction. In addition to the characteristic peak of the isovector giant dipole resonance (IVGDR) at  $\approx 15$  MeV, among several dipole states in the low-energy region between 7 MeV and 10 MeV that are characterized by single particle transitions, at  $\approx 8.5$  MeV a single pronounced peak is found with a more distributed structure of the RQRPA amplitude, exhausting 3.3% of the TRK sum rule. As we have shown in Ref. [22] by analyzing the corresponding transition densities, the dynamics of this low-energy mode is very different from that of the IVGDR: the proton and neutron transition densities are in phase in the nuclear interior, there is almost no contribution from the protons in the surface region, the isoscalar transition density dominates over the isovector one in the interior, and the large neutron component in the surface region contributes to the formation of a node in the isoscalar transition density. The low-lying pygmy dipole resonance (PDR) does not belong to statistical E1 excitations sitting

on the tail of the GDR, but represents a fundamental structure effect: the neutron skin oscillates against the core. In the right panel of Fig. 2 we compare the RQRPA results for the Sn isotopes with experimental data on IVGDR excitation energies [34]. The energy of the resonance  $E_{\text{GDR}}$  is defined as the centroid energy  $\bar{E} = m_1/m_0$ , calculated in the same energy window as the one used in the experimental analysis (13–18 MeV). The GDR excitation energies decrease with increasing mass number, but the mass dependence is not monotonic. The calculation predicts an increase of the GDR excitation energy at the  $N = 82$  shell closure. We notice that for the four isotopes for which data have been reported, the calculated energies of the GDR are in excellent agreement with the experimental values.

In Fig. 3 the calculated peak energies of the PDR in Sn isotopes are plotted as function of the mass number. The RQRPA predicts a monotonic decrease of the PDR with mass number, and only a small kink in the calculated excitation energies is found at the  $N = 82$  shell closure. In the same plot we have also included the calculated one-neutron separation energies, in comparison with the experimental data and the extrapolated value from the compilation of Audi and Wapstra [35]. The self-consistent RHB calcula-

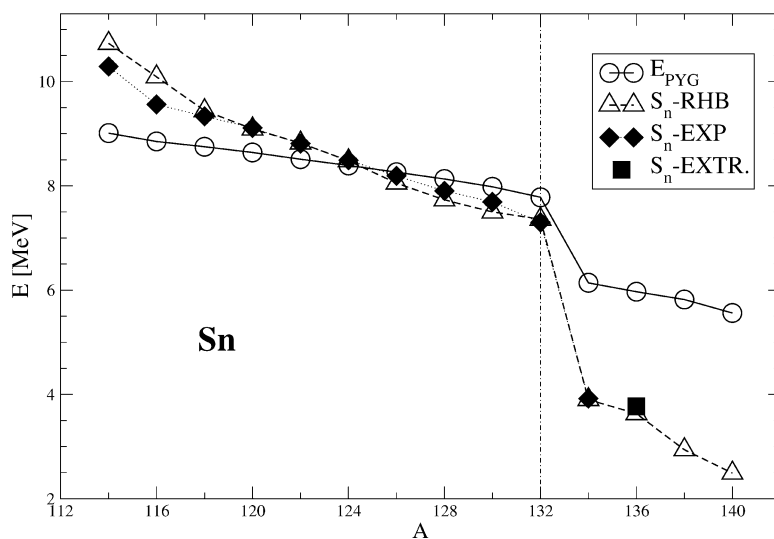


Fig. 3. The calculated PDR peak energies and the one-neutron separation energies for the sequence of Sn isotopes, as functions of the mass number. The DD-ME1 effective interaction has been used in the RHB and RQRPA calculations. The RHB results for the neutron separation energies are compared with the experimental and extrapolated values [35].

tion, with the DD-ME1 mean-field effective interaction and the D1S Gogny pairing force, reproduces in detail the one-neutron separation energies of the Sn nuclei. We notice that the separation energies decrease much faster than the calculated PDR excitation energies. At  $N = 82$ , in particular, the separation energies display a sharp decrease, whereas the shell closure produces only a weak effect on the PDR excitation energies. The important result here is that for  $A < 124$  the PDR excitation energies are lower than the corresponding one-neutron separation energies, whereas for  $A \geq 124$  the pygmy resonance is located above the neutron emission threshold. This means, of course, that in the latter case the observation of the PDR in  $(\gamma, \gamma')$  experiments will be strongly hindered. One would naively expect that, in a given isotopic chain, the relative strength of the PDR increases monotonically with the number of neutrons, at least within a major shell. In Ref. [22] we have shown, however, that in the case of Sn isotopes the PDR peak is most pronounced in  $^{124}\text{Sn}$ . A combination of shell effects and reduced pairing correlations, decrease the relative strength of the PDR in heavier Sn nuclei below  $N = 82$ .

Besides being intrinsically interesting as an exotic mode of excitation, the occurrence of the PDR might have important implications for the r-process nucleo-

synthesis. Namely, although the E1 strength of the PDR is small compared to the total dipole strength, if located well below the neutron separation energy the PDR can significantly enhance the radiative neutron capture cross section on neutron-rich nuclei, as shown in recent large-scale QRPA calculations of the E1 strength for the whole nuclear chart [2,3]. The results of the present RHB + QRPA calculation show, however, that in very neutron-rich nuclei the PDR could be located well above the neutron emission threshold (see also Fig. 4).

It is, of course, interesting to explore other isotopic chains of spherical nuclei where one expects, or has already observed, the occurrence of the PDR in the E1 excitation spectrum. In Fig. 4 we plot the calculated PDR excitation energies and the one-neutron separation energies for the Ni and Pb isotopic chains. As in the case of Sn isotopes, in Pb nuclei the PDR strength is always concentrated in one peak and we display the corresponding peak energies. On the other hand, Ni nuclei are much lighter and the PDR strength is fragmented over several states. Therefore, the excitation energies shown in the left panel of Fig. 4 correspond to the centroid energies of the PDR strength distributions. The RHB results for the neutron separation energies are compared with the experimental values [35]. For both chains the RQRPA calculation predicts

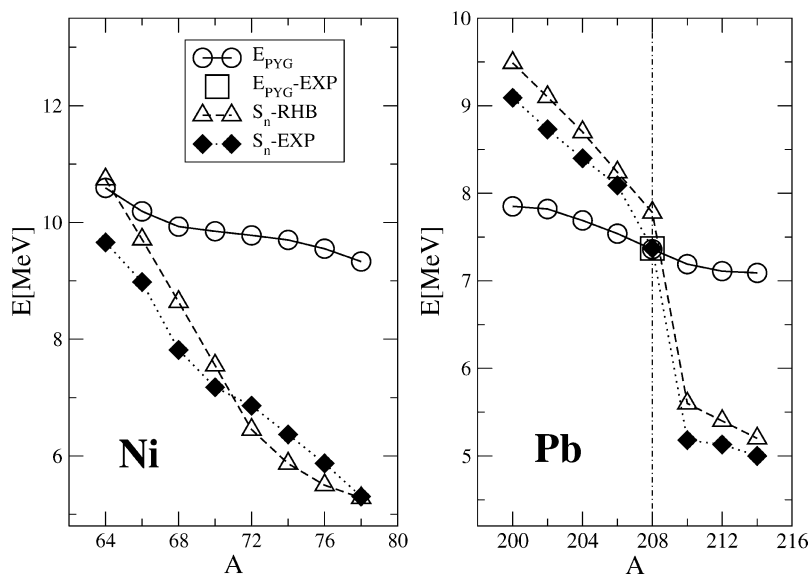


Fig. 4. Same as in Fig. 3, but for the Ni and Pb isotopic chains. The open square denotes the experimental position of the PDR in  $^{208}\text{Pb}$  [9].

a very weak mass dependence of the PDR excitation energies. In the sequence of Ni isotopes the crossing between the theoretical curves of one-neutron separation energies and PDR excitation energies is calculated already at  $A = 64$ . In heavier, neutron-rich Ni nuclei the PDR is expected to be located high above the neutron emission threshold. Notice that for the Ni isotopic chain the agreement between the calculated and experimental neutron separation energies is not as good as for the Sn nuclei and, therefore, the actual point of crossing between the PDR and the one-neutron separation energy could occur for  $A < 64$ . The Ni isotopes are not very rigid nuclei and, for a more quantitative prediction, one would probably have to go beyond the simple mean-field plus QRPA calculation and include correlation effects. For the Pb isotopes the crossing point is calculated at  $A = 208$ , in excellent agreement with very recent experimental data on the PDR in  $^{208}\text{Pb}$  [9]. Future  $(\gamma, \gamma')$  experiments on Pb nuclei could confirm the predictions of the present analysis.

In conclusion, we have employed the self-consistent RHB model and the RQRPA in the analysis of the isotopic dependence of the excitation energies of the PDR in the Ni, Sn, and Pb isotopic chains. By using the density-dependent DD-ME1 meson-exchange effective interaction, which reproduces available data on

the charge radii, the neutron skin, and neutron separation energies, we have shown that the RQRPA results for the excitation energies of the isovector giant dipole resonances are in excellent agreement with data in Sn nuclei. We have then compared the isotopic dependence of the excitation energies of the PDR with that of the corresponding one-neutron separation energies. The separation energies decrease much faster with mass number. Especially at shell closures the one-neutron separation energies display a sharp decrease, whereas only a weak discontinuity is predicted for the PDR peak energies. In all three isotopic chains the RQRPA predicts a crossing between the curves of neutron separation energies and PDR excitation energies already at moderate proton–neutron asymmetry. For the heavier isotopes the PDR is calculated above the neutron emission threshold, and this will effectively preclude the observation of the PDR in  $(\gamma, \gamma')$  experiments on very neutron-rich nuclei.

### Acknowledgements

This work has been supported in part by the Bundesministerium für Bildung und Forschung under project 06 MT 193, and by the Gesellschaft für Schwe-

rionenforschung (GSI) Darmstadt. N.P. acknowledges support from the Deutsche Forschungsgemeinschaft (DFG) under contract SFB 634.

## References

- [1] S. Goriely, Phys. Lett. B 436 (1998) 10.
- [2] S. Goriely, E. Khan, Nucl. Phys. A 706 (2002) 217.
- [3] S. Goriely, E. Khan, M. Samyn, Nucl. Phys. A 739 (2004) 331.
- [4] D.C. Radford, et al., Phys. Rev. Lett. 88 (2002) 222501.
- [5] J. Terasaki, J. Engel, W. Nazarewicz, M. Stoitsov, Phys. Rev. C 66 (2002) 054313.
- [6] A. Leistenschneider, et al., Phys. Rev. Lett. 86 (2001) 5442.
- [7] T. Hartmann, J. Enders, P. Mohr, K. Vogt, S. Volz, A. Zilges, Phys. Rev. Lett. 85 (2000) 274.
- [8] K. Govaert, et al., Phys. Rev. C 57 (1998) 2229.
- [9] N. Ryezayeva, et al., Phys. Rev. Lett. 89 (2002) 272502.
- [10] J. Enders, et al., Nucl. Phys. A 724 (2003) 243.
- [11] A. Zilges, S. Volz, M. Babilon, T. Hartmann, P. Mohr, K. Vogt, Phys. Lett. B 542 (2002) 43.
- [12] Y. Suzuki, K. Ikeda, H. Sato, Prog. Theor. Phys. 83 (1990) 180.
- [13] J. Chambers, E. Zaremba, J.P. Adams, B. Castel, Phys. Rev. C 50 (1994) R2671.
- [14] H. Sagawa, T. Suzuki, Phys. Rev. C 59 (1999) 3116.
- [15] P.G. Reinhard, Nucl. Phys. A 649 (1999) 305c.
- [16] G. Coló, P.F. Bortignon, Nucl. Phys. A 696 (2001) 427.
- [17] M. Tohyama, A.S. Umar, Phys. Lett. B 516 (2001) 415.
- [18] M. Matsuo, Nucl. Phys. A 696 (2001) 371.
- [19] N. Tsoneva, H. Lenske, Ch. Stoyanov, Nucl. Phys. A 731 (2004) 273.
- [20] N. Tsoneva, H. Lenske, Ch. Stoyanov, Phys. Lett. B 586 (2004) 213.
- [21] D. Vretenar, N. Paar, P. Ring, G.A. Lalazissis, Nucl. Phys. A 692 (2001) 496.
- [22] N. Paar, P. Ring, T. Nikšić, D. Vretenar, Phys. Rev. C 67 (2003) 034312.
- [23] Z.Y. Ma, N. Van Giai, A. Wandelt, D. Vretenar, P. Ring, Nucl. Phys. A 686 (2001) 173.
- [24] D. Vretenar, N. Paar, T. Nikšić, P. Ring, Phys. Rev. C 65 (2002) 021301.
- [25] D. Vretenar, N. Paar, T. Nikšić, P. Ring, Phys. Rev. Lett. 91 (2003) 262502.
- [26] T. Nikšić, D. Vretenar, P. Ring, Phys. Rev. C 66 (2002) 064302.
- [27] T. Nikšić, D. Vretenar, P. Finelli, P. Ring, Phys. Rev. C 66 (2002) 024306.
- [28] J.F. Berger, M. Girod, D. Gogny, Nucl. Phys. A 428 (1984) 23c.
- [29] P.G. Reinhard, M. Rufa, J. Maruhn, W. Greiner, J. Friedrich, Z. Phys. 323 (1996) 13.
- [30] G.A. Lalazissis, J. König, P. Ring, Phys. Rev. C 55 (1997) 540.
- [31] E.G. Nadiakov, K.P. Marinova, Yu.P. Gangrsky, At. Data Nucl. Data Tables 56 (1994) 133.
- [32] F. Le Blanc, et al., Eur. Phys. J. A 15 (2002) 49.
- [33] A. Krasznahorkay, et al., Phys. Rev. Lett. 82 (1999) 3216.
- [34] B.L. Berman, S.C. Fultz, Rev. Mod. Phys. 47 (1975) 713.
- [35] G. Audi, A.H. Wapstra, Nucl. Phys. A 595 (1995) 409.